

Dissipation in mesoscale superfluids

Adrian Del Maestro^{1,*} and Bernd Rosenow²

¹*Department of Physics, University of Vermont, Burlington, VT 05405, USA*

²*Institut für Theoretische Physik, Universität Leipzig, D-04103, Leipzig, Germany*

We investigate the maximum speed at which a driven superfluid can flow through a narrow constriction with a size on the order of the healing length. Considering dissipation via the thermal nucleation of quantized vortices, we calculate the critical velocity for superfluid ⁴He and ultracold atomtronic circuits, identify fundamental length and velocity scales, and are thus able to present results obtained in widely different temperature and density ranges in a universal framework. For ultra-narrow channels we predict a drastic reduction in the critical velocity as the energy barrier for flow reducing thermally activated phase slip fluctuations is suppressed.

The flow of dissipationless atomic supercurrents in neutral superfluids is one of the most dramatic manifestations of macroscopic quantum coherence [1–3], with applications to matter wave interferometry [4–6]. Recently, there has been increased interest in dimensionally confined superfluids, due to progress in manufacturing nanoscale channels and fountain effect devices for studying the flow of superfluid helium [7–24] and the availability of trapped non-equilibrium atomic Bose-Einstein condensates [25–39]. Common to these experiments in vastly different density and interaction regimes is an observed increase in dissipation for highly confined systems.

In general, superflow is possible at speeds less than a superfluid critical velocity set by the Landau criterion $v_c \leq \min \varepsilon(p)/p$ below which there are no accessible excitations $\varepsilon(p)$ with momentum p [40]. Among the different types of excitations in superfluids, quantized vortices [1, 41–44] give rise to the smallest v_c . For flow through a cylindrical channel, if the total kinetic energy is converted into vortex rings with the size a of the constriction, the Landau criterion predicts a critical velocity $v_{c,F} \sim (\kappa/a) \ln(a/\xi_0)$ [42] where $\kappa = h/m$ is the quantum of circulation for condensed bosons of mass m and ξ_0 is a characteristic length scale of the superfluid. This prediction (due to Feynman) has been born out by nearly a half-century worth of superfluid massflow observations with *temperature independent* critical velocities [2, 45]. However, it must ultimately break down as the constriction radius approaches ξ_0 . Moreover, any observed temperature dependence of v_c can only be described by the existence of an energy activation barrier for the creation of vortices.

In this letter, we consider confined mesoscale superflow through quasi-one-dimensional (1d) constrictions with a characteristic size a approaching the temperature (T) dependent correlation (healing) length $\xi(T)$, and find a strong increase in dissipation when $a/\xi(T)$ approaches one. Going beyond previous studies [2, 36], we (i) quantitatively predict the temperature, size, and drive depen-

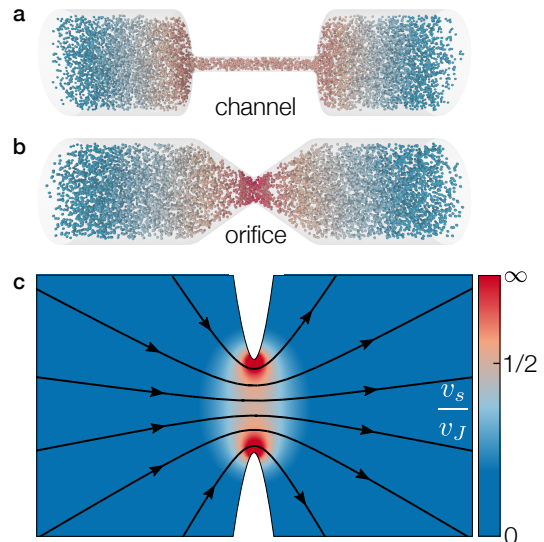


Figure 1. **a** A current of superfluid atoms driven through a long channel with a homogeneous (radius independent) flow profile. **b** Flow through a narrow orifice formed from the surface of revolution of a hyperbola around the flow axis. **c** Velocity field \mathbf{v}_s for the potential flow through an orifice in units of the average flow speed v_J . The flow direction is indicated by black lines, with the magnitude diverging as a power law at the orifice boundary [46].

dence of the critical velocity without adjustable parameters, (ii) use a paradigmatic orifice geometry to model the enhancement of vortex creation in spatially inhomogeneous flow near a sharp boundary, which significantly lowers critical velocities, (iii) point out the universality between high density ⁴He [8, 18] and low density atomic condensates [25, 27, 28, 36], by characterizing constrictions via the dimensionless length a/ξ and measuring velocities in units of $v_0 = \kappa/(4\pi\xi_0)$, and (iv) describe the crossover to the purely 1d limit, a Luttinger liquid in the thermal regime. Predictions are expected to be logarithmically accurate in the critical regime while corrections of order unity may arise when extrapolating to lower T .

We begin by considering superflow between reservoirs with a chemical potential difference $\Delta\mu$ (pressure differ-

* Adrian.DelMaestro@uvm.edu

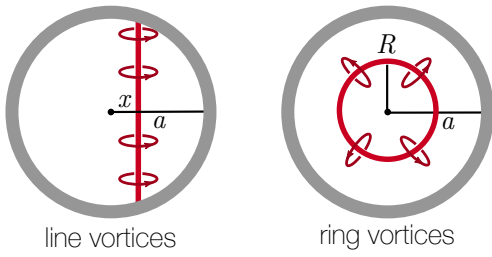


Figure 2. Two vortex types that can be nucleated in a confined geometry. Left: A line vortex located a distance x from the center of the orifice or channel. The vortex line begins and ends on the boundary, with the flow circulating around it. Right: A vortex line can detach from the boundary and close on itself forming a vortex ring of radius R . Arrows indicate the circulation of quantized flow around the vortex core.

ence ΔP) connected by prototypical geometric constrictions with either a “channel” or “orifice” shape as seen in Fig. 1. Channel flow is spatially homogeneous with a constant superfluid velocity v_s that is representative of flow through long narrow cylindrical pores. Flow through an orifice can be studied by considering a hyperbolic surface of revolution connecting two bulk reservoirs where the potential flow problem can be solved analytically [46]. The solution is characterized by divergent flow near the boundaries as seen in Fig. 1c, where the creation of line vortices (Fig. 2 left) is facilitated. Ring vortices in the center of the orifice (Fig. 2 right) are not strongly affected by the spatial dependence of flow near the boundaries.

The energy cost for creating a quantized vortex is due to (i) the kinetic energy of circular superflow around the core region, and (ii) the loss of condensation energy within the core [41]. For a vortex ring of radius R (length $\mathcal{L} = 2\pi R$) or a line vortex (length \mathcal{L}) in a constriction of radius a , the combination of these effects yields

$$E_{\text{tension}} = \frac{\mathcal{L}}{4\pi} \rho_s \kappa^2 \left[\ln \frac{\ell}{\xi} + \alpha \right] \quad (1)$$

where $\ell = a$ for line vortices, $\ell = R$ for ring vortices, and the constant α depends of the vortex type and model of the core. Solving the Gross-Pitaevski (GP) equation, one finds that $\alpha = 0.385$ for line vortices [47] and $\alpha = \ln 8 - 2 + 0.385 \simeq 0.464$ for ring vortices [48]. Obtaining a more accurate model of the vortex core is possible via numerical simulations in low [49] and high density superfluids [50, 51]. The results are consistent with the GP value of α and show only weak density dependence. The reduction of the kinetic energy of superflow due to interaction with the vortex is

$$E_{\text{flow}} = \kappa \rho_s \iint \mathbf{v}_s \cdot d\mathbf{S} \quad , \quad (2)$$

where the integral is over the area bounded by the vortex ring, or between the vortex line and boundary. The total

energy is $E = E_{\text{tension}} + E_{\text{flow}}$. To unify the description of driven quantum fluids, we employ the Josephson relation in 3d [52] $\kappa^2 \rho_s(T) \xi(T) = 4\pi^2 k_B T_c$ where $\rho_s(T)$ is the superfluid mass density for a transition temperature T_c and $\xi(T) = \xi_0 (1 - T/T_c)^{-\nu}$ and ν is the correlation length critical exponent. We numerically checked that the Josephson relation is valid to within 20% down to $T/T_c \approx 0.7$, for details see [46]. For flow through an orifice with speed v_J , we obtain the energy barrier for a line vortex located a distance x from its center:

$$\beta_c E_{\text{line}}(x) = 2\pi \frac{a}{\xi} \sqrt{1 - \left(\frac{x}{a}\right)^2} \left[\ln \left(1 - \frac{|x|}{a}\right) + \ln \frac{a}{\xi} + \alpha \right] - \frac{v_J}{v_0} \left(\frac{a}{\xi}\right)^2 \frac{\pi^2 \xi}{2\xi_0} \left(1 - \frac{x}{a}\right). \quad (3)$$

and that for a centered ring vortex with radius R :

$$\beta_c E_{\text{ring}}(R) = 2\pi^2 \frac{R}{\xi} \left(\ln \frac{R}{\xi} + \alpha \right) - \frac{v_J}{v_0} \left(\frac{a}{\xi}\right)^2 \frac{\pi^2 \xi}{\xi_0} \left[1 - \sqrt{1 - \left(\frac{R}{a}\right)^2} \right] \quad (4)$$

where $\beta_c = 1/(k_B T_c)$. From these expressions (and those for channel flow derived in the supplementary material [46]) we observe the emergence of natural length (ξ_0) and velocity ($v_0 = \kappa/(4\pi\xi_0)$) scales that are essential for constructing a universal theory of dissipative superfluids.

The velocity of superflow at finite T is limited by the thermal nucleation of quantized vortices which traverse the flow lines leading to a change of phase of the superfluid order parameter by $\pm 2\pi$, (see e.g. Ref. [53]). The decay of a persistent current is then governed by vortex energetics via:

$$\Gamma = \Gamma_0 \left[e^{-\beta E_{\text{max}}(+v_J)} - e^{-\beta E_{\text{max}}(-v_J)} \right] \quad , \quad (5)$$

where $h\Gamma = \Delta\mu = m\Delta P/\rho_s$ drives total mass flow $J = \rho_s \iint \mathbf{v}_s \cdot d\mathbf{S} \equiv \pi a^2 \rho_s v_J$ and $E_{\text{max}} \equiv \max_{\mathcal{L}} E$ is the saddle point of the vortex excitation energy over the domain of the channel or orifice. The difference of rates in Eq. (5) corresponds to the contributions from vortices which reduce and increase the superflow, respectively. The attempt rate Γ_0 is related to the phase space available for vortex excitations and is geometry dependent:

$$\Gamma_0 = \frac{1}{\tau_{GL}} \frac{La}{\xi^2} \begin{cases} \frac{\pi a}{\xi} & \text{vortex ring} \\ 2\pi & \text{vortex line} \end{cases} \quad , \quad (6)$$

with $\tau_{GL}^{-1} = 16k_B(T_c - T)/h$ the Ginzburg-Landau relaxation rate. The decay rate in Eq. (5) contains the main contribution from integration over zero modes, corresponding to a translation of the vortex with action S_v in both time and space. In addition, there are Jacobians due to the change of coordinates from the superfluid phase Φ

to the radius R of the vortex ring or the location x of the vortex line, and a contribution from integration over the negative eigenvalue mode. As previously discussed [54, 55], the Jacobian is $\sqrt{S_v/2\pi}$ for the zero modes, and the negative eigenvalue mode contributes a factor of similar magnitude. We have verified that the combination of all these factors is of order unity and thus neglect them. Other modifications to the pre-factor in Eq. (5) could result when considering the microscopic details of dynamics and vortex evolution inside the constriction [56–61] and would introduce quantitative logarithmic corrections to the nucleation theory.

Evaluation of the critical velocity from Eq. (5) proceeds as follows. For a given flow profile and vortex type, we maximize the vortex energy as a function of $\pm v_J$ over the spatial domain of possible configurations. This leads to critical vortex positions $x^*(\pm v_J) \in (-a, a)$ for line vortices and critical radii $R^*(\pm v_J) \in (0, a)$ for ring vortices. Vortices with a length smaller than the critical one will tend to collapse, or annihilate at boundaries, while those larger can proliferate, leading to dissipation. For a fixed constriction radius a/ξ_0 , temperature T/T_c and external drive potential Γ_0/Γ , Eq. (5) can be numerically solved self-consistently giving the critical velocity when $v_J = v_c$.

When $a/\xi_0 \gg 1$, the boundaries of the constriction no longer play an important role and only uniform channel flow is relevant. Due to the resulting large critical velocities, energy increasing fluctuations can be neglected and the saddle point energies can be found analytically. The resulting pair of transcendental equations

$$\frac{R^*}{\xi} = \frac{1}{\pi^2} \frac{T}{T_c} \frac{\ln \frac{\Gamma_0}{\Gamma}}{\ln \frac{R^*}{\xi} + \alpha - 1} \quad (7)$$

$$\frac{v_c}{v_0} = \frac{\xi_0}{R^*} \left(\ln \frac{R^*}{\xi} + \alpha + 1 \right) \quad (8)$$

can be solved numerically for R^* and v_c [46].

Our main results for the critical velocity in both the channel and orifice flow profiles are shown as lines in Fig. 3. When employing the scales v_0 and ξ_0 , mass flow measurements in drastically different density, interaction, and temperature regimes are well bounded by the vortex nucleation theory, and experiments on confined superfluid ^4He and low-dimensional Bose-Einstein condensates can be directly compared. For both flow profiles, line vortices have lower activation energies than ring vortices, giving smaller velocities and a lower bound on v_c . An absolute upper bound is provided by ring vortices in the orifice flow profile. In the limit $a \gg \xi_0$, where the geometry approaches that of bulk flow, we recover the intrinsic superfluid velocity due to the nucleation of vortex rings analyzed by Langer and Fisher [43]. For ^4He , we have used a vortex core size determined from specific heat measurements [46, 63], and have thus been able to correct a long-standing inconsistency of 27 orders of magnitude in the applied pressure difference employed in Ref. [43]

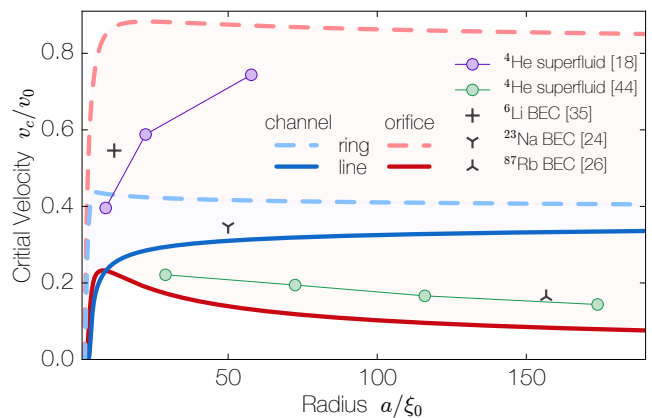


Figure 3. Upper and lower bounds on the critical velocity are indicated by lines from the channel ($L = 10^3 \xi_0$, blue) and orifice ($L = 10 \xi_0$, red) flow profiles for both ring (dashed) and line vortices (solid) at $T = 0.7T_c$, $\hbar\Gamma = 0.1k_B T_c$ and $\nu \simeq 0.6717$. Symbols show experimental massflow results for superfluid helium [18, 45] and Bose-Einstein condensates [25, 27, 36]. Details are provided in the supplemental information [46] where we discuss the relationship between the zero temperature healing length and ξ_0 in the weakly interacting Bose gas [62].

to obtain agreement with experiments. For tight constrictions, both the lower and upper bound turn towards smaller velocities indicative of enhanced dissipation.

While details of additional experiments are discussed in the supplemental material [46], Fig. 3 includes data from two ^4He studies whose critical velocities display a clear temperature dependence – a signature of activated behavior. Harrison *et al.* [45] measured flow in networks of imperfect pores of varying radii which should provide a lower bound on flow speeds, behavior consistent with our results. Recent measurements on single nanopores by Duc *et al.* [18] exhibit drastically different behavior: large critical velocities that *decrease* as the radius approaches the correlation length. While the microscopic details of the flow profiles are not known, v_c for the narrowest pore is bounded by the channel prediction, consistent with the reported aspect ratio of 10:1 and suggesting a crossover to strongly dissipative quasi-1d flow.

Fig. 3 also includes results from analogous neutral atomtronic circuits using ultracold bosonic and fermionic condensates [3]. Here, the “orifice” can be replaced with a quantum point contact between two resonantly coupled Fermi gases [37] or channel-like flow can be driven by the discharge of a bosonic atom capacitor [29] or by dragging an optical potential through a simply [27, 36] or multiply connected [28, 30, 33] Bose-Einstein condensate. For the latter, our nucleation theory yields $v_c \approx 100 \mu\text{m/s}$ for the drag and $v_c \approx 1 \text{ mm/s}$ for the toroidal flow in remarkable agreement with measurements and more microscopic theoretical analysis [33, 35, 64].

Intuition for the dissipation in narrow pores with radius $a \approx \xi$ can be gained by considering the unoptimized energy of line vortices with position $x = 0$ at the center of the channel. This approximation is qualitatively correct since narrow pores can be expected to be in the channel flow regime with line vortex activation energies comparable to temperature. The vortex energy is found from the sum of Eqs. (1) and (2) with $x = 0$:

$$\beta_c E_{\text{line}}(x=0) = 2\pi \frac{a}{\xi} \left(\ln \frac{a}{\xi} + \alpha \right) - \frac{\pi^2 \xi v_s}{2\xi_0 v_0} \left(\frac{a}{\xi} \right)^2, \quad (9)$$

with resulting critical velocity

$$\frac{v_c}{v_0} = \frac{2}{\pi^2} \frac{\xi \xi_0}{a^2} \frac{T}{T_c} \sinh^{-1} \left\{ \frac{1}{64\pi a L} \frac{\xi^2}{\left(1 - \frac{T}{T_c}\right)^{-1}} \right. \\ \left. \times \exp \left[\frac{2\pi a T_c}{\xi} \left(\ln \frac{a}{\xi} + \alpha \right) \right] \right\}. \quad (10)$$

As $a/\xi \rightarrow 1^+$, the activation energy in the exponent of Eq. (10) decreases rapidly, and the small multiplier of the exponential is no longer compensated. As a consequence, the critical velocity drops by several orders of magnitude.

In the quasi-1d ($a \lesssim \xi$) limit there are no transverse degrees of freedom, and the system can be described in analogy to fluctuating superconducting wires by computing the resistance due to thermally activated phase slips [65, 66]. Translated into the language of 1d superfluidity, the phase slip energy is (see supplemental material [46]):

$$\beta_c E_{1d} = \pi \left(\frac{a}{\xi} \right)^2 \left[\frac{4}{3\sqrt{2}} - \pi \frac{\xi v_s}{\xi_0 v_0} \right]. \quad (11)$$

For line vortices in the channel flow profile, the tension scales with $(a/\xi)^2$ in contrast to the linear dependence in Eq. (9). This difference is unimportant at the crossover $a/\xi \approx 1$ and the critical velocity from the nucleation of line vortices and the 1d theory should be in agreement as demonstrated in Fig. 4a. The lower bound on the critical velocity due to line vortices drops three orders of magnitude, and crosses over to the 1d result for single mode channels. An analogous crossover from the linear to non-linear Josephson junction regime has been observed in superflow through an array of orifices near T_c [8].

Fig. 4b shows the T -dependence of v_c for constrictions with $a/\xi_0 = 10$ and we observe a reduction as $T \rightarrow T_c$. Qualitatively, this is due to the fact that $\xi(T)$ increases as $T \rightarrow T_c$, thus reducing the ratio $a/\xi(T)$ which determines the effective constriction radius. Experiments on ^4He have reported an apparent temperature power-law scaling of v_c [18] which we have confirmed is the spurious result of an interplay between the thermal activation energy and vortex attempt rate. As $T \rightarrow 0$, vortices will no longer be thermally activated and dissipation will be dominated by the nucleation of quantum phase slips [67, 68].

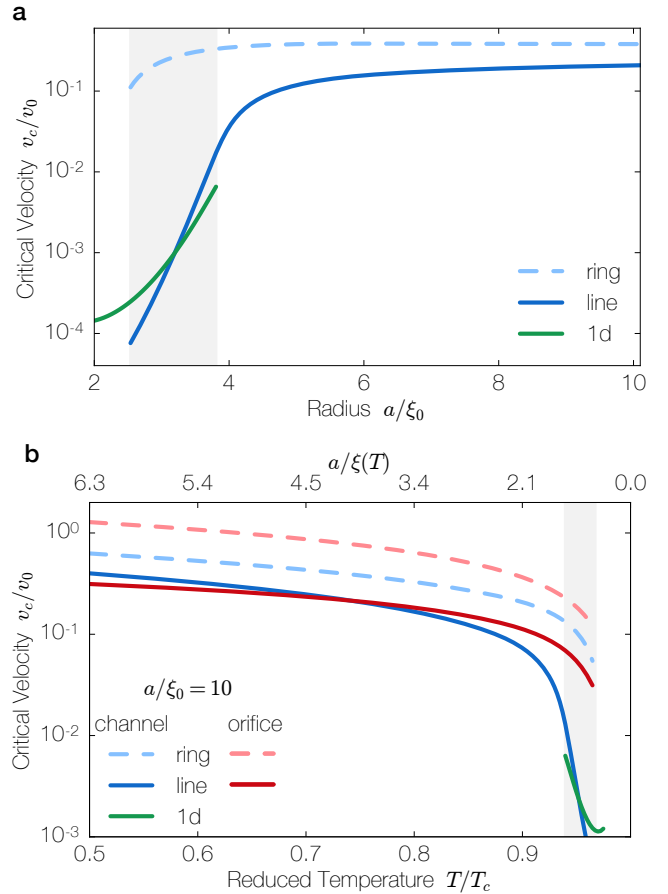


Figure 4. **a** The critical velocity in a quasi-1d superfluid channel of length $L = 10^3 \xi_0$ as a function of radius for $T/T_c = 3/4$, $h\Gamma = k_B T_c$ and $\xi(3T_c/4) \simeq 2.5\xi_0$. The solid and dashed blue lines extending over the full domain of the plot were computed via the vortex nucleation theory, while the green line is for 1d, Eq. (11). **b** The temperature dependence of the critical velocity for a channel ($L = 10^3 \xi_0$) and orifice ($L = 10 \xi_0$) with $a = 10\xi_0$. As $T \rightarrow T_c$, the correlation length ξ diverges, thus reducing the effective channel width $a/\xi(T)$ and lowering v_c . The shaded gray bars demarcates the radii where $1 \leq a/\xi(T) \leq 3/2$ and in this region the upper bound due to ring vortices is no longer expected to be relevant.

In summary, we considered two characteristic confined flow geometries and the thermal activation of representative low energy excitations, ring and line vortices, inside them. The resulting bounds they place on the critical velocity of neutral superflow through narrow constrictions agree with a large body of measurements on confined superfluid ^4He and low-dimensional ultracold gases. As the confinement radius approaches the healing length, we find an exponential suppression of the critical velocity of three orders of magnitude. The experimental observation of this dramatic reduction would be a clear signal of entering the strongly fluctuating mesoscale regime.

Acknowledgements – We thank B.I. Halperin, G. Ger-

vais, P.F. Duc, P. Taborek and K. Wright for helpful discussions. A.D. appreciates the University of Leipzig's hospitality and his participation in a grand challenges workshop on quantum fluids and solids supported by NSF DMR-1523582. B.R. acknowledges support by DFG grant No. RO 2247/8-1.

-
- [1] P. Anderson, "Considerations on the Flow of Superfluid Helium," *Rev. Mod. Phys.* **38**, 298 (1966).
- [2] Eric Varoquaux, "Anderson's considerations on the flow of superfluid helium: Some offshoots," *Rev. Mod. Phys.* **87**, 803 (2015).
- [3] Chih-Chun Chien, Sebastiano Peotta, and Massimiliano Di Ventra, "Quantum transport in ultracold atoms," *Nature Phys.* **11**, 998 (2015).
- [4] Yuki Sato and Richard Packard, "Superfluid helium interferometers," *Phys. Today* **65**, 31 (2012).
- [5] T. Schumm, S. Hofferberth, L. M. Andersson, S. Wildermuth, S. Groth, I. Bar-Joseph, J. Schmiedmayer, and P. Kruger, "Matter-wave interferometry in a double well on an atom chip," *Nat Phys* **1**, 57–62 (2005).
- [6] Sheng-wei Chiow, Tim Kovachy, Hui-Chun Chien, and Mark A. Kasevich, " $102\hbar k$ large area atom interferometers," *Phys. Rev. Lett.* **107**, 130403 (2011).
- [7] E. Hoskinson, R. E. Packard, and M. Haard, Thomas, "Oscillatory motion: Quantum whistling in superfluid helium-4," *Nature* **433**, 376 (2005).
- [8] E. Hoskinson, Y. Sato, I. Hahn, and R. E. Packard, "Transition from phase slips to the Josephson effect in a superfluid ^4He weak link," *Nature Phys.* **2**, 23 (2005).
- [9] Zhi Gang Cheng, John Beamish, Andrew D. Fefferman, Fabien Souris, Sébastien Balibar, and Vincent Dauvois, "Helium mass flow through a solid-superfluid-solid junction," *Phys. Rev. Lett.* **114**, 165301 (2015).
- [10] Zhi Gang Cheng and John Beamish, "Compression-driven mass flow in bulk solid ^4He ," *Phys. Rev. Lett.* **117**, 025301 (2016).
- [11] Y. Vekhov, W. J. Mullin, and R. B. Hallock, "Universal temperature dependence, flux extinction, and the role of ^3He impurities in superfluid mass transport through solid ^4He ," *Phys. Rev. Lett.* **113**, 035302 (2014).
- [12] Y. Vekhov and R. B. Hallock, "Mass Flux Characteristics in Solid ^4He for $T > 100$ mK: Evidence for Bosonic Luttinger-Liquid Behavior," *Phys. Rev. Lett.* **109**, 045303 (2012).
- [13] M. W. Ray and R. B. Hallock, "Mass flux and solid growth in solid ^4He for 60–700 mk," *Phys. Rev. Lett.* **105**, 145301 (2010).
- [14] M. W. Ray and R. B. Hallock, "Observation of unusual mass transport in solid hcp ^4He ," *Phys. Rev. Lett.* **100**, 235301 (2008).
- [15] M. Boninsegni, A. B. Kuklov, L. Pollet, N. V. Prokof'ev, B. V. Svistunov, and M. Troyer, "Luttinger liquid in the core of a screw dislocation in helium-4," *Phys. Rev. Lett.* **99**, 035301 (2007).
- [16] M. Savard, G. Dauphinais, and G. Gervais, "Hydrodynamics of superfluid helium in a single nanohole," *Phys. Rev. Lett.* **107**, 254501 (2011).
- [17] M. Savard, C. Tremblay-Darveau, and G. Gervais, "Flow conductance of a single nanohole," *Phys. Rev. Lett.* **103**, 104502 (2009).
- [18] Pierre-Francois Duc, Michel Savard, Matei Petrescu, Bernd Rosenow, Adrian Del Maestro, and Guillaume Gervais, "Critical flow and dissipation in a quasi-one-dimensional superfluid," *Science Adv.* **1**, e1400222 (2015).
- [19] A. E. Velasco, S. G. Friedman, M. Pevarnik, Z. S. Siwy, and P. Taborek, "Pressure-driven flow through a single nanopore," *Phys. Rev. E* **86**, 025302 (2012).
- [20] A. E. Velasco, C. Yang, Z. S. Siwy, M. E. Toimil-Molares, and P. Taborek, "Flow and evaporation in single micrometer and nanometer scale pipes," *Applied Physics Lett.* **105**, 033101 (2014).
- [21] Jeffrey Botimer and Peter Taborek, "Pressure driven flow of superfluid ^4He through a nanopipe," *Phys. Rev. Fluids* **1**, 054102 (2016).
- [22] D. V. Fil and S. I. Shevchenko, "Relaxation of superflow in a network: Application to the dislocation model of supersolidity of helium crystals," *Phys. Rev. B* **80**, 100501 (2009).
- [23] Adrian Del Maestro, Massimo Boninsegni, and Ian Affleck, " ^4He luttinger liquid in nanopores," *Phys. Rev. Lett.* **106**, 105303 (2011).
- [24] Lode Pollet and Anatoly B. Kuklov, "Topological quantum phases of ^4He confined to nanoporous materials," *Phys. Rev. Lett.* **113**, 045301 (2014).
- [25] C. Raman, M. Köhl, R. Onofrio, D. S. Durfee, C. E. Kulewicz, Z. Hadzibabic, and W. Ketterle, "Evidence for a Critical Velocity in a Bose-Einstein Condensed Gas," *Phys. Rev. Lett.* **83**, 2502 (1999).
- [26] Gentaro Watanabe, F. Dalfovo, F. Piazza, L. P. Pitaevskii, and S. Stringari, "Critical velocity of superfluid flow through single-barrier and periodic potentials," *Phys. Rev. A* **80**, 053602 (2009).
- [27] T. W. Neely, E. C. Samson, A. S. Bradley, M. J. Davis, and B. P. Anderson, "Observation of Vortex Dipoles in an Oblate Bose-Einstein Condensate," *Phys. Rev. Lett.* **104**, 160401 (2010).
- [28] A. Ramanathan, K. C. Wright, S. R. Muniz, M. Zelan, W. T. Hill, C. J. Lobb, K. Helmerson, W. D. Phillips, and G. K. Campbell, "Superflow in a Toroidal Bose-Einstein Condensate: An Atom Circuit with a Tunable Weak Link," *Phys. Rev. Lett.* **106**, 130401 (2011).
- [29] Jeffrey G. Lee, Brian J. McIlvain, C. J. Lobb, and Hill W. T., "Analogues of Basic Electronic Circuit Elements in a Free-Space Atom Chip," *Sci. Rep.* **3**, 1034 (2013).
- [30] K. C. Wright, R. B. Blakestad, C. J. Lobb, W. D. Phillips, and G. K. Campbell, "Driving Phase Slips in a Superfluid Atom Circuit with a Rotating Weak Link," *Phys. Rev. Lett.* **110**, 025302 (2013).
- [31] Noel Murray, Michael Krygier, Mark Edwards, K. C. Wright, G. K. Campbell, and Charles W. Clark, "Probing the circulation of ring-shaped Bose-Einstein condensates," *Phys. Rev. A* **88**, 053615 (2013).
- [32] K. C. Wright, R. B. Blakestad, C. J. Lobb, W. D. Phillips, and G. K. Campbell, "Threshold for creating excitations in a stirred superfluid ring," *Phys. Rev. A* **88**, 063633 (2013).
- [33] Stephen Eckel, Jeffrey G Lee, Fred Jendrzejewski, Noel Murray, Charles W Clark, Christopher J Lobb, William D Phillips, Mark Edwards, and Gretchen K Campbell, "Hysteresis in a quantized superfluid 'atomtronic' circuit," *Nature* **506**, 200 (2014).
- [34] F Jendrzejewski, S Eckel, N Murray, C Lanier, M Ed-

- wards, C J Lobb, and G K Campbell, “Resistive Flow in a Weakly Interacting Bose-Einstein Condensate,” *Phys. Rev. Lett.* **113**, 045305 (2014).
- [35] Amy C. Mathey, Charles W. Clark, and L. Mathey, “Decay of a superfluid current of ultracold atoms in a toroidal trap,” *Phys. Rev. A* **90**, 023604 (2014).
- [36] Wolf Weimer, Kai Morgener, Vijay Pal Singh, Jonas Siegl, Klaus Hueck, Niclas Luick, Ludwig Mathey, and Henning Moritz, “Critical Velocity in the BEC-BCS Crossover,” *Phys. Rev. Lett.* **114**, 095301 (2015).
- [37] Dominik Husmann, Shun Uchino, Sebastian Krinner, Martin Lebrat, Thierry Giamarchi, Tilman Esslinger, and Jean-Philippe Brantut, “Connecting strongly correlated superfluids by a quantum point contact,” *Science* **350**, 1498 (2015).
- [38] Vijay Pal Singh, Wolf Weimer, Kai Morgener, Jonas Siegl, Klaus Hueck, Niclas Luick, Henning Moritz, and Ludwig Mathey, “Probing superfluidity of Bose-Einstein condensates via laser stirring,” *Phys. Rev. A* **93**, 023634 (2016).
- [39] Aijun Li, Stephen Eckel, Benjamin Eller, Kayla E Warren, Charles W Clark, and Mark Edwards, “Superfluid transport dynamics in a capacitive atomtronic circuit,” (2016), 1606.02758.
- [40] L. Landau, “Theory of the Superfluidity of Helium II,” *Phys. Rev.* **60**, 356–358 (1941).
- [41] S. V. Iordanskii, “Vortex ring formation in a superfluid,” *Sov. Phys. JETP* **21**, 467 (1965).
- [42] R. P. Feynman, “Application of quantum mechanics to liquid helium,” in *Prog. in Low Temp. Phys.*, Vol. 1 (Amsterdam, 1955).
- [43] J. Langer and Michael Fisher, “Intrinsic Critical Velocity of a Superfluid,” *Phys. Rev. Lett.* **19**, 560 (1967).
- [44] G. E. Volovik, “Quantum-mechanical formation of vortices in a superfluid liquid,” *Sov. Phys. JETP* **58**, 458 (1972).
- [45] S. J. Harrison and K. Mendelssohn, “Superfluid 4He Velocities in Narrow Channels between 1.8 and 0.3 K,” in *Low Temperature Physics*, edited by T D Timmerhaus (Springer, New York, 1974) p. 298.
- [46] See Supplemental Material for details on potential flow, vortex energies, experimental comparisons, and the critical velocity in the $a/\xi \gg 1$ and $a/\xi \approx 1$ limits.
- [47] L. P. Pitaevskii, “Vortex lines in an imperfect Bose gas,” *Sov. Phys. JETP* **13**, 451 (1961).
- [48] P. H. Roberts and J. Grant, “Motions in a Bose condensate. I. The structure of the large circular vortex,” *J. Phys. A: Gen. Phys.* **4**, 55 (1971).
- [49] T. Winiecki, J. F. McCann, and C. S. Adams, “Vortex structures in dilute quantum fluids,” *Europhys. Lett.* **48**, 475 (1999).
- [50] Gerardo Ortiz and David M Ceperley, “Core Structure of a Vortex in Superfluid He4,” *Phys. Rev. Lett.* **75**, 4642 (1995).
- [51] D. E. Galli, L. Reatto, and M. Rossi, “Quantum Monte Carlo study of a vortex in superfluid 4He and search for a vortex state in the solid,” *Phys. Rev. B* **89**, 224516 (2014).
- [52] B. D. Josephson, “Relation between the superfluid density and order parameter for superfluid He near T_c ,” *Phys. Lett.* **21**, 608 (1966).
- [53] J. S. Langer, “Theory of Nucleation Rates,” *Phys. Rev. Lett.* **21**, 973 (1968).
- [54] Sidney Coleman, “Fate of the false vacuum: Semiclassical theory,” *Phys. Rev. D* **15**, 2929 (1977); Curtis G. Callan Jr. and Sidney Coleman, “Fate of the false vacuum. II. First quantum corrections,” *ibid.* **16**, 1762 (1977).
- [55] L. S. Schulman, *Techniques and Applications of Path Integration* (Wiley and Sons, New York, 1981).
- [56] Aurel Bulgac, Yuan-Lung Luo, Piotr Magierski, Kenneth J Roche, and Yongle Yu, “Real-Time Dynamics of Quantized Vortices in a Unitary Fermi Superfluid,” *Science* **332**, 1288–1291 (2011).
- [57] Tarik Yefsah, Ariel T Sommer, Mark J H Ku, Lawrence W Cheuk, Wenjie Ji, Waseem S Bakr, and Martin W Zwierlein, “Heavy solitons in a fermionic superfluid,” *Nature* **499**, 426–430 (2013).
- [58] Mark J H Ku, Wenjie Ji, Biswaroop Mukherjee, Elmer Guardado-Sanchez, Lawrence W Cheuk, Tarik Yefsah, and Martin W Zwierlein, “Motion of a Solitonic Vortex in the BEC-BCS Crossover,” *Phys. Rev. Lett.* **113**, 065301 (2014).
- [59] Simone Donadello, Simone Serafini, Marek Tylutki, Lev P Pitaevskii, Franco Dalfovo, Giacomo Lamporesi, and Gabriele Ferrari, “Observation of Solitonic Vortices in Bose-Einstein Condensates,” *Phys. Rev. Lett.* **113**, 065302 (2014).
- [60] S Serafini, M Barbiero, M Debortoli, S Donadello, F Larcher, F Dalfovo, G Lamporesi, and G Ferrari, “Dynamics and Interaction of Vortex Lines in an Elongated Bose-Einstein Condensate,” *Phys. Rev. Lett.* **115**, 170402 (2015).
- [61] Mark J. H. Ku, Biswaroop Mukherjee, Tarik Yefsah, and Martin W. Zwierlein, “Cascade of Solitonic Excitations in a Superfluid Fermi gas: From Planar Solitons to Vortex Rings and Lines,” *Phys. Rev. Lett.* **116**, 045304 (2016).
- [62] Nikolay Prokof’ev, Oliver Ruebenacker, and Boris Svistunov, “Weakly interacting Bose gas in the vicinity of the normal-fluid-superfluid transition,” *Phys. Rev. A* **69**, 053625 (2004).
- [63] Alan Singasaas and Guenter Ahlers, “Universality of static properties near the superfluid transition in He4,” *Phys. Rev. B* **30**, 5103 (1984).
- [64] M. Crescimanno, C. G. Koay, R. Peterson, and R. Walsworth, “Analytical estimate of the critical velocity for vortex pair creation in trapped Bose condensates,” *Phys. Rev. A* **62**, 063612 (2000).
- [65] J. Langer and Vinay Ambegaokar, “Intrinsic Resistive Transition in Narrow Superconducting Channels,” *Phys. Rev.* **164**, 498 (1967).
- [66] D. McCumber and B. Halperin, “Time Scale of Intrinsic Resistive Fluctuations in Thin Superconducting Wires,” *Phys. Rev. B* **1**, 1054 (1970).
- [67] S. Khlebnikov, “Quasiparticle Scattering by Quantum Phase Slips in One-Dimensional Superfluids,” *Phys. Rev. Lett.* **93**, 090403 (2004).
- [68] Ipei Danshita, “Universal Damping Behavior of Dipole Oscillations of One-Dimensional Ultracold Gases Induced by Quantum Phase Slips,” *Phys. Rev. Lett.* **111**, 025303 (2013).

Supplementary material for “Dissipation in mesoscale superfluids”

VELOCITY FLOW PROFILES

As illustrated in Fig. 1a-b of the main text, we consider two different superfluid flow profiles through long narrow *channels*, and hole-like *orifices*.

Channel Flow

For a long cylindrical channel of radius a and length $L \gg a$ oriented with its axis along the z -direction we neglect any acceleration of the fluid at the entry and exit to obtain a spatially independent velocity field

$$\mathbf{v}_s = v_J \hat{z} = \frac{J}{\pi a^2 \rho_s} \hat{z} \quad (\text{S1})$$

where J is the total mass flow rate and ρ_s is the superfluid mass density.

Orifice Flow

The geometry of an orifice of radius a oriented in the $x-y$ plane centered at the origin can be conveniently described in oblate spheroidal coordinates (ζ, η, ϕ) by the surface $\eta = 0$ where

$$\begin{aligned} x &= a \cos \phi \sqrt{(1 + \zeta^2)(1 - \eta^2)} \\ y &= a \sin \phi \sqrt{(1 + \zeta^2)(1 - \eta^2)} \\ z &= a \zeta \eta . \end{aligned} \quad (\text{S2})$$

In general, $\phi \in [0, 2\pi)$, $\zeta \in [0, \infty)$ and $\eta \in [-1, 1)$ with the surface $|\eta| = \eta_0$ corresponding to a hyperboloid of revolution about the y -axis (see Fig. 1b). Steady incompressible flow through the orifice with total rate J can be studied by defining a potential field $\Phi(\zeta, \eta, \phi)$ such that $\mathbf{v}_s = (\hbar/m)\nabla\Phi$ and solving $\nabla^2\Phi = 0$ by requiring that Φ is continuous at $\zeta = 0$, and subject to the boundary condition that the velocity component perpendicular to the surface defined by $\eta = 0$ vanishes outside the orifice. This yields the velocity field: [S1–S3]

$$\mathbf{v}_s = \frac{v_J}{2} \frac{1}{\sqrt{(\zeta^2 + \eta^2)(\zeta^2 + 1)}} \hat{\zeta} \quad (\text{S3})$$

which is plotted in the $y-z$ plane in Fig. 1c. Inside the orifice at $\zeta = 0$ this expression simplifies to:

$$\mathbf{v}_s(r, z = 0) = \frac{v_J}{2\sqrt{1 - r^2/a^2}} \hat{z} \quad (\text{S4})$$

which diverges near the boundary as $r \rightarrow a$.

VORTEX ENERGIES

Employing Eqs. (1)–(2) in the main text in combination with the spatial dependence of v_s we may now obtain the energy cost of nucleating line and ring vortices.

Channel Flow

For channels, we use the velocity profile in Eq. (S1).

Line Vortices

For a line vortex attached to the walls of a channel of radius a offset a distance x from the center with length $\mathcal{L}(x) = 2\sqrt{a^2 - x^2}$ as seen in Fig. 2 the total energy is the sum of $E_{\text{tension}} + E_{\text{flow}}$ and given by:

$$E_{\text{line}}(x) = \frac{\kappa^2 \rho_s}{2\pi} \sqrt{a^2 - x^2} \left(\ln \frac{a - |x|}{\xi} + \alpha \right) - \kappa \rho_s v_J \left[a^2 \cos^{-1} \left(\frac{x}{a} \right) - x \sqrt{a^2 - x^2} \right]. \quad (\text{S5})$$

Now, the superfluid density and correlation length ξ can be related via the Josephson scaling relation in three dimensions [S4]

$$\xi(T) = \frac{4\pi^2 k_B T_c}{\kappa^2 \rho_s(T)} \quad (\text{S6})$$

where $\xi(T) = \xi_0(1 - T/T_c)^{-\nu}$. Fig. S1 shows the accuracy of this relation for superfluid ^4He [S5] and a weakly interacting Bose gas [S6] down to $T/T_c \approx 0.7$. All temperature dependence now enters expressions through the

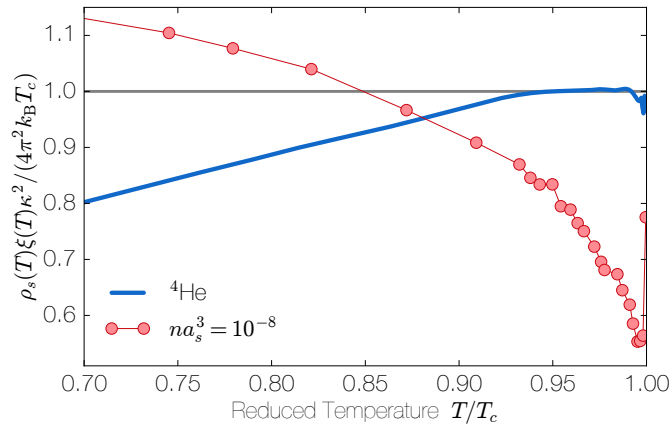


Figure S1. The accuracy of the Josephson scaling relation defined in Eq. (S6) compared with experimental results for the superfluid density and correlation length at saturated vapor pressure from Ref. [S5] for ^4He and theoretical results for a weakly interacting Bose gas with $na^3 = 10^{-8}$ (data adapted from Ref. [S6]) where we have replaced the scaling prefactor ξ_0 with the healing length ξ_n . See section III.B for details. Here n is the number density and a_s the scattering length.

correlation length and the resulting dimensionless vortex energy is given by:

$$\beta_c E_{\text{line}}(x) = 2\pi \frac{a}{\xi} \sqrt{1 - \left(\frac{x}{a}\right)^2} \left[\ln \left(1 - \frac{|x|}{a} \right) + \ln \frac{a}{\xi} + \alpha \right] - \frac{v_J}{v_0} \left(\frac{a}{\xi} \right)^2 \frac{\pi \xi}{\xi_0} \left[\cos^{-1} \left(\frac{x}{a} \right) - \frac{x}{a} \sqrt{1 - \left(\frac{x}{a}\right)^2} \right] \quad (\text{S7})$$

with $\beta_c \equiv 1/(k_B T_c)$ and we have identified the fundamental velocity scale $v_0 = \kappa/(4\pi\xi_0)$. This expression simplifies to Eq. (9) in the main text when the vortex line is located at the center of the channel $x = 0$.

Ring Vortices

For a ring vortex of radius R , with length $\mathcal{L} = 2\pi R$ the energy can be written as:

$$E_{\text{ring}}(R) = \frac{1}{2} \kappa^2 \rho_s R \left(\ln \frac{R}{\xi} + \alpha \right) - \kappa \rho_s \pi R^2 v_J \quad (\text{S8})$$

yielding

$$\beta_c E_{\text{ring}}(R) = 2\pi^2 \frac{R}{\xi} \left(\ln \frac{R}{\xi} + \alpha \right) - \frac{v_J}{v_0} \left(\frac{R}{\xi} \right)^2 \frac{\pi^2 \xi}{\xi_0}. \quad (\text{S9})$$

Orifice Flow

For the orifice flow profile, the velocity field now has the spatial dependence seen in Eq. (S4) and Fig. 1c with a divergence at the boundary. While the effective line tension E_{tension} (first term) in Eqs. (S5) and (S8) are unchanged, a modified spatial integral in E_{flow} needs to be computed.

Line Vortices

The energy cost for flow captured by a line vortex at position x is given by

$$E_{\text{flow,line}}(x) = \frac{\pi}{2} \kappa \rho_s v_J a^2 \left(1 - \frac{x}{a} \right) \quad (\text{S10})$$

leading to the total dimensionless vortex energy:

$$\begin{aligned} \beta_c E_{\text{line}}(x) = & 2\pi \frac{a}{\xi} \sqrt{1 - \left(\frac{x}{a} \right)^2} \left[\ln \left(1 - \frac{|x|}{a} \right) + \ln \frac{a}{\xi} + \alpha \right] \\ & - \frac{v_J}{v_0} \left(\frac{a}{\xi} \right)^2 \frac{\pi^2 \xi}{2\xi_0} \left(1 - \frac{x}{a} \right). \end{aligned} \quad (\text{S11})$$

Ring Vortices

For ring vortices, the flow integral is given by

$$E_{\text{flow,ring}}(R) = \kappa \rho_s v_J \pi a^2 \left[1 - \sqrt{1 - \left(\frac{R}{a} \right)^2} \right] \quad (\text{S12})$$

which leads to

$$\begin{aligned} \beta_c E_{\text{ring}}(R) = & 2\pi^2 \frac{R}{\xi} \left(\ln \frac{R}{\xi} + \alpha \right) \\ & - \frac{v_J}{v_0} \left(\frac{a}{\xi} \right)^2 \frac{\pi^2 \xi}{\xi_0} \left[1 - \sqrt{1 - \left(\frac{R}{a} \right)^2} \right]. \end{aligned} \quad (\text{S13})$$

APPLICATION TO MASS FLOW EXPERIMENTS

In this section we provide a more complete analysis of neutral bosonic mass flow experiments that were discussed in Fig. 3 of the main text.

Superfluid Helium-4

A recent review by Varoquaux [S7] includes a compilation of superfluid critical velocity results from a diverse set of experiments (both dependent and independent of temperature) that are reproduced in Fig. S2 along with theoretical upper and lower bounds computed within the vortex nucleation theory using parameters relevant for superfluid helium. The experimental data from Ref. [S7] can be grouped into two distinct regions. For larger channels, a temperature

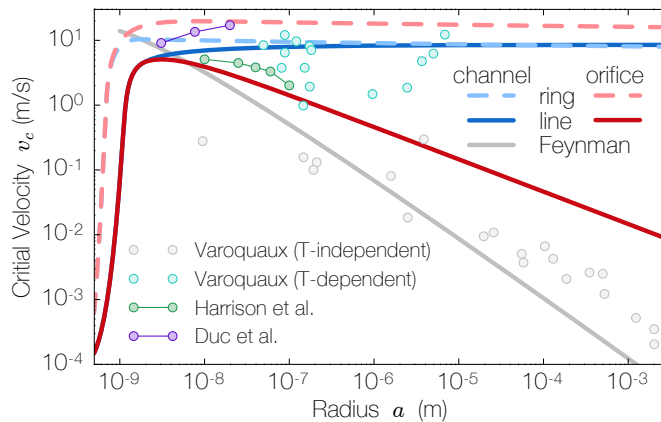


Figure S2. A compilation of experimental results on the critical superfluid velocity v_c of ^4He under pressure driven flow through constrictions with radius a from Varoquaux (temperature independent and dependent) [S7], Harrison *et al.* [S8] and Duc *et al.* [S9]. The temperature independent results for larger channels are qualitatively described by the Feynman critical velocity $v_{c,F} = (\kappa/4\pi a) \ln(2a/\xi_0)$ where $\xi_0 \simeq 3.45 \text{ \AA}$ is the zero temperature coherence length. For smaller pores with larger temperature dependent critical velocities, the data is well-bounded by the predictions of the vortex nucleation theory for ring and line vortices in the orifice and channel flow profiles with $L = 30 \text{ nm}$ and $\Gamma = 4 \text{ GHz}$ at $T = 1.5 \text{ K}$, values consistent with those in the experiment [S9], and representative for the other experiments.

Reference	System	v_c (mm/s)	v_0 (mm/s)	a (μm)	ξ_0 (μm)	T/T_c
Neely <i>et al.</i> [S10]	^{87}Rb	0.2	1.2	47	0.3	0.6
Ramanathan <i>et al.</i> [S11]	^{23}Na	0.9	0.7	7	0.51	0.2
Raman <i>et al.</i> [S12]	^{23}Na	1.6	4.6	15	0.3	0.8
Weimer <i>et al.</i> [S13]	^6Li (molecule)	1.7	3.1	10	0.85	0.5

Table I. Critical velocity and related velocity, length and temperature scales extracted from four neutral bosonic mass flow experiments in ultracold atomic and molecular condensates.

independent critical velocity increases as the channel size is reduced (grey circles). This is consistent with the Feynman prediction $v_F \sim \kappa/a$, where vortex rings are dynamically ejected from the end of the channel.

A second group of temperature dependent critical velocities in pores with radii $a \sim 100 \text{ nm} - 10 \mu\text{m}$ have considerably larger velocities and are in a thermally activated dissipation regime that is well bounded by the vortex nucleation theory. Additionally, Fig. S2 includes a systematic set of experiments performed by Harrison and Mendelssohn [S8] (green circles) employing the fountain effect to drive superfluid mass flow through arrays of $10^4 - 10^7 L = 5 \mu\text{m}$ pores etched in irradiated mica using HF acid with radii $a = 20, 50, 80, 120$ and 200 nm . These results, taken at $T = 1.5 \text{ K}$, should be considered as representing a lower bound on the critical velocity as all pores were assumed to be open in the analysis and both a variation in radii and a taper along the channel were observed.

Experiments by Duc *et al.* [S9] shown in Fig. S2 are in the interesting mesoscopic regime where $a/[\xi_0(1-T/T_c)^{-\nu}] \sim O(1)$. For superfluid helium, $\xi_0 \simeq 3.45 \text{ \AA}$, $T_c = T_\lambda \simeq 2.1768 \text{ K}$ and $\nu \simeq 0.6717$. They observed a decrease in the critical velocity as the pore radius was reduced. In these experiments, ^4He mass flow is studied through single pores nanofabricated using a transmission electron beam incident on a $L \simeq 30 \text{ nm}$ thick silicon nitride wafer resulting in smooth constrictions with radii $a \simeq 3.14, 7.81$ and 20 nm . Critical velocities were reported for $T = 1.5 \text{ K}$, and flow was driven via pressure differences between $\Delta P = 250 - 830 \text{ mbar}$ which corresponds to an external drive frequency $\Gamma \simeq 2 - 7 \text{ GHz} \sim k_B T_c/h$.

Ultracold Gases

In systems of neutral ultracold atoms, flow is driven by dynamically shaping an optical potential which causes a local imbalance in the chemical potential (see Ref. [S14] for current experimental designs). For dilute gases, the prefactor ξ_0 which appears in the critical scaling relation for the correlation length can be related to the zero temperature healing length $\xi_h = 1/\sqrt{8\pi a_s n}$ via known universal results for the weakly interacting Bose gas [S6]. Here n is the number density and a_s is the scattering length and provided that $na^3 \ll 10^{-5}$ the superfluid density can be written in terms of a universal scaling function f_s :

$$\rho_s(t) = \frac{16\pi^3 mn}{[\zeta(\frac{3}{2})]^{4/3}} (na^3)^{1/3} (1-t)^2 f_s(t, na^3) \quad (\text{S14})$$

where m is the mass, $t = 1 - T/T_c$ is the reduced temperature and the Riemann zeta function, $\zeta(3/2)$, appears through the use of the critical temperature of the non-interacting Bose gas: $k_B T_c = (2\pi\hbar^2/m)[n/\zeta(3/2)]^{2/3}$. The function f_s is known from high precision Monte Carlo calculations [S6, S15] and when $t \ll 1$, $f_s \propto (t/\sqrt[3]{na^3})^\nu$. Writing the temperature dependent correlation length in the critical region as $\xi(T) = (\xi_0/\xi_h)\xi_h t^{-\nu}$, we can use the Josephson relation in Eq. (S6) to determine

$$\frac{\xi_0}{\xi_h} = \mathcal{A} (na^3)^{(2\nu-1)/6} \quad (\text{S15})$$

where $\mathcal{A} \simeq 3.8$ is a universal number. Thus, for experimentally accessible weakly interacting Bose gases $\xi_0 \simeq \mathcal{B}\xi_h$ with $\mathcal{B} \sim 1 - 2$. Away from the critical region, the full scaling function can be used to test the accuracy of the Josephson relation with the result shown in Fig. S1.

Thus, to analyze non-equilibrium mass flow experiments employing ultracold Bose-Einstein condensates, we approximate $\xi_0 \approx \xi_h \sim 1 \mu\text{m}$, which yields the critical velocity scale $v_0 = \hbar/(4\pi m \xi_0) \sim 1 \text{ mm/s}$. In Fig. 3 of the main text, we have shown results for the critical velocity from three ultracold gas experiments using the parametrization shown in Table I. We have not included the low temperature data point from Ref. [S11] where the errors in our critical theory are difficult to estimate. We find that the other experiments are in the same flow regime as tightly confined superfluid helium.

INTRINSIC CRITICAL VELOCITY OF BULK SUPERFLUIDS

In the $a \gg \xi_0$ limit we can directly find the critical ring vortex radius R^* that maximizes the energy barrier in the constant channel flow profile in Eq. (S8) as

$$\frac{R^*}{\xi} = \frac{v_0}{v_J} \frac{\xi_0}{\xi} \left(\ln \frac{R^*}{\xi} + \alpha + 1 \right). \quad (\text{S16})$$

In this bulk regime, one only needs to consider the effects of vortices which reduce the total energy and Eq. (5) gives

$$\begin{aligned} \ln \frac{\Gamma_0}{\Gamma} &= \beta E_{\text{ring}}(R^*) \\ &= \frac{T_c}{T} \left[2\pi^2 \frac{R^*}{\xi} \left(\ln \frac{R^*}{\xi} + \alpha \right) - \frac{v_c}{v_0} \left(\frac{R^*}{\xi} \right)^2 \frac{\pi^2 \xi}{\xi_0} \right] \end{aligned} \quad (\text{S17})$$

which can be solved for the critical velocity v_c . Combining Eq. (S17) with Eq. (S16) with $v_J = v_c$ gives the transcendental equation

$$\frac{R^*}{\xi} = 2 \frac{\ln \frac{R^*}{\xi} + \alpha - \frac{1}{2\pi^2} \frac{T}{T_c} \ln \frac{\Gamma_0}{\Gamma}}{\ln \frac{R^*}{\xi} + \alpha + 1} \quad (\text{S18})$$

which can be simplified to yield Eq. (7). Replacing $\ln \Gamma_0/\Gamma$ in Eq. (S17) via Eq. (S18) we obtain the critical velocity in the large radius limit in Eq. (8).

Eq. (7) in the main text is equivalent to Eq. (13) in Langer and Fisher [S16] (LF), noting the change of variables $\eta_c \equiv \ln 8R^*/\xi$, their use of a rigid vortex core with $\alpha = \ln 8 - 7/4$ and setting $\ln \Gamma_0/\Gamma \simeq 83$. The un-physically large

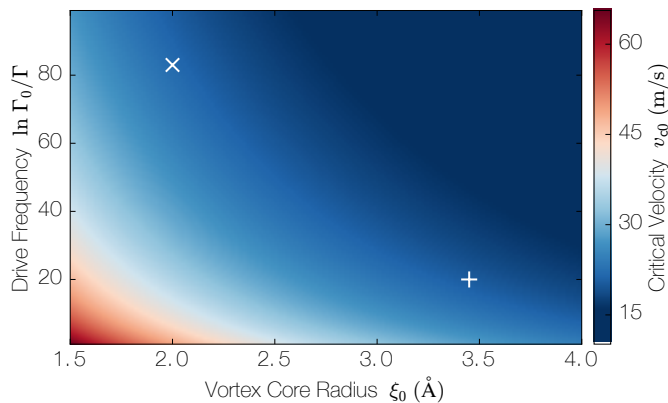


Figure S3. The intrinsic critical velocity scale v_{c0} of superfluid ^4He as a function of the effective zero temperature core size ξ_0 and external drive frequency $\ln \Gamma_0/\Gamma$. In order to obtain a physically meaningful value of the critical velocity $v_c = v_{c0}(1-T/T_c)^\nu$ when using $\xi_0 = 2 \text{ \AA}$, Langer and Fisher [S16] had to consider an extremal value for the external drive as indicated by the cross (\times). When utilizing a larger core size of $\xi_0 = 3.45 \text{ \AA}$ as experimentally determined in Ref. [S17], $\ln \Gamma_0/\Gamma$ can be reduced to more physically meaningful values as indicated by the plus (+).

value of $\ln \Gamma/\Gamma_0$ employed by LF was required to ensure that their computed value of $v_c = v_{c0}(1-T/T_c)^\nu$ in the scaling regime was below the absolute upper bound given by the Landau criterion. In order to understand the origin of this long-standing discrepancy, we have investigated v_{c0} as a function of both the external drive Γ_0/Γ and vortex core details ξ_0 with the results shown in Fig. S3.

THE ONE-DIMENSIONAL LIMIT

To derive Eq. (11) in the main text, we begin with a free energy functional near T_c :

$$f = f_0 + \frac{\hbar^2}{2m} |\nabla \Psi|^2 + A |\Psi|^2 + \frac{B}{2} |\Psi|^4 \quad (\text{S19})$$

where f_0 is a condensate energy density and the wave function is given by: $\Psi(\mathbf{r}) = \sqrt{n(\mathbf{r})} e^{i\Phi(\mathbf{r})}$ with $n(\mathbf{r})$ the number density. In a spatially homogeneous superfluid, the free energy is minimized when $|\Psi|^2 \equiv n_0 = -A/B$. Substituting this value for the field into Eq. (S19):

$$f - f_0 = -\frac{A^2}{2B} = -\frac{H_c^2}{8\pi}, \quad (\text{S20})$$

where the last equality is schematic and in analogy to superconductors where H_c is the critical field. Identifying $-A/B$ with the density and performing the usual rescaling: $\tilde{\Psi} = \Psi/\sqrt{n_0}$ one introduces the correlation length $\xi(T)$ such that $\xi^2(T) = \hbar^2/2mA(T)$, and we can now write $f - f_0 = \rho_s \kappa^2 / 16\pi^2 \xi^2(T)$. According to Refs. [S18-S19], the free energy barrier of a phase slip excitation inside a quasi-one-dimensional channel of cross-sectional area πa^2 is given by

$$\Delta F_0 = \frac{8\sqrt{2}}{3} \frac{H_c^2}{8\pi} A \xi = \frac{\sqrt{2}}{6\pi} \rho_s \kappa^2 \xi \left(\frac{a}{\xi} \right)^2. \quad (\text{S21})$$

The energy reduction due to a superflow J is $\delta F = \kappa \rho_s v_J \pi a^2$, and adding the free energy barrier Eqs. (S21) one obtains the total phase slip energy in Eq. (11) of the main text. The total phase slip rate is $\Gamma = 2\Gamma_0 e^{-\Delta F_0/k_B T} \sinh(\delta F/k_B T)$, and solving for v_c we find

$$\begin{aligned} \frac{v_c}{v_0} &= \frac{1}{\pi} \left(\frac{\xi_0}{a} \right) \frac{T}{T_c} \left(1 - \frac{T}{T_c} \right)^{-\nu} \\ &\times \sinh^{-1} \left[\frac{\Gamma}{2\Gamma_0} \exp \left(\frac{4\pi}{3\sqrt{2}} \frac{a^2}{\xi_0^2} \frac{T_c}{T} \left(1 - \frac{T}{T_c} \right)^{2\nu} \right) \right], \end{aligned} \quad (\text{S22})$$

where [S19]

$$\Gamma_0 = \frac{aL}{\xi_0^2} \left(1 - \frac{T}{T_c}\right)^{2\nu+1} \left(\frac{2\sqrt{2}\pi T_c}{3T}\right)^{1/2} \frac{8k_B T_c}{\pi\hbar}. \quad (\text{S23})$$

Eq. (S22) is shown in Fig. 4 of the main text.

-
- [S1] P.M.C. Morse and H. Feshbach, *Methods of Theoretical Physics*, Vol. 2 (McGraw-Hill, 1953).
- [S2] E Blount and C Varma, “Hydrodynamics of vortex generation in flowing superfluid helium,” *Phys. Rev. B* **14**, 2888 (1976).
- [S3] K W Schwarz, “Phase slip and phase-slip cascades in He4superflow through a small orifice,” *Phys. Rev. Lett.* **71**, 259 (1993).
- [S4] B. D. Josephson, “Relation between the superfluid density and order parameter for superfluid He near T_c ,” *Phys. Lett.* **21**, 608 (1966).
- [S5] R J Donnelly and C F Barenghi, “The observed properties of liquid helium at the saturated vapor pressure,” *J. Phys. Chem.* **27**, 1217 (1998).
- [S6] Nikolay Prokof’ev, Oliver Ruebenacker, and Boris Svistunov, “Weakly interacting Bose gas in the vicinity of the normal-fluid-superfluid transition,” *Phys. Rev. A* **69**, 053625 (2004).
- [S7] Eric Varoquaux, “Anderson’s considerations on the flow of superfluid helium: Some offshoots,” *Rev. Mod. Phys.* **87**, 803 (2015).
- [S8] S. J. Harrison and K. Mendelssohn, “Superfluid 4He Velocities in Narrow Channels between 1.8 and 0.3 K,” in *Low Temperature Physics*, edited by T D Timmerhaus (Springer, New York, 1974) p. 298.
- [S9] Pierre-Francois Duc, Michel Savard, Matei Petrescu, Bernd Rosenow, Adrian Del Maestro, and Guillaume Gervais, “Critical flow and dissipation in a quasi-one-dimensional superfluid,” *Science Adv.* **1**, e1400222 (2015).
- [S10] T. W. Neely, E. C. Samson, A. S. Bradley, M. J. Davis, and B. P. Anderson, “Observation of Vortex Dipoles in an Oblate Bose-Einstein Condensate,” *Phys. Rev. Lett.* **104**, 160401 (2010).
- [S11] A. Ramanathan, K. C. Wright, S. R. Muniz, M. Zelan, W. T. Hill, C. J. Lobb, K. Helmerson, W. D. Phillips, and G. K. Campbell, “Superflow in a Toroidal Bose-Einstein Condensate: An Atom Circuit with a Tunable Weak Link,” *Phys. Rev. Lett.* **106**, 130401 (2011).
- [S12] C. Raman, M. Köhl, R. Onofrio, D. S. Durfee, C. E. Kuklewicz, Z. Hadzibabic, and W. Ketterle, “Evidence for a Critical Velocity in a Bose-Einstein Condensed Gas,” *Phys. Rev. Lett.* **83**, 2502 (1999).
- [S13] Wolf Weimer, Kai Morgener, Vijay Pal Singh, Jonas Siegl, Klaus Hueck, Niclas Luick, Ludwig Mathey, and Henning Moritz, “Critical Velocity in the BEC-BCS Crossover,” *Phys. Rev. Lett.* **114**, 095301 (2015).
- [S14] Chih-Chun Chien, Sebastiano Peotta, and Massimiliano Di Ventra, “Quantum transport in ultracold atoms,” *Nature Phys.* **11**, 998 (2015).
- [S15] B Capogrosso-Sansone, S Giorgini, S. Pilati, L Pollet, N Prokof’ev, B Svistunov, and M. Troyer, “The Beliaev technique for a weakly interacting Bose gas,” *New J. Phys.* **12**, 043010 (2010).
- [S16] J. Langer and Michael Fisher, “Intrinsic Critical Velocity of a Superfluid,” *Phys. Rev. Lett.* **19**, 560 (1967).
- [S17] Alan Singasaas and Guenter Ahlers, “Universality of static properties near the superfluid transition in He4,” *Phys. Rev. B* **30**, 5103 (1984).
- [S18] J. Langer and Vinay Ambegaokar, “Intrinsic Resistive Transition in Narrow Superconducting Channels,” *Phys. Rev.* **164**, 498 (1967).
- [S19] D. McCumber and B. Halperin, “Time Scale of Intrinsic Resistive Fluctuations in Thin Superconducting Wires,” *Phys. Rev. B* **1**, 1054 (1970).